

RESEARCH ARTICLE

Soluble guanylate cyclase stimulation reduces oxidative stress in experimental Chronic Obstructive Pulmonary Disease

Tanja Paul¹, Anna Salazar-Degracia², Victor I. Peinado^{1,3*}, Olga Tura-Ceide^{1,3}, Isabel Blanco^{1,3}, Esther Barreiro^{2,3}, Joan A. Barberà^{1,3}

1 Department of Pulmonary Medicine, Hospital Clínic, *Institut d'Investigacions Biomèdiques August Pi i Sunyer* (IDIBAPS), University of Barcelona, Barcelona, Spain, **2** Pulmonology Department-Lung Cancer and Muscle Research group, IMIM-Hospital del Mar, Health and Experimental Sciences Department (CEXS), Universitat Pompeu Fabra (UPF), Barcelona Biomedical Research Park (PRBB), Barcelona, Spain, **3** Biomedical Research Networking Center on Respiratory Diseases (CIBERES), Madrid, Spain

* vpeinado@clinic.ub.es



Abstract

Objective

Soluble guanylate cyclase (sGC) is a key enzyme of the nitric oxide–cyclic guanosine 3',5'-monophosphate (NO–cGMP) signaling pathway, and its pharmacological stimulation has been shown to prevent the development of emphysema and pulmonary vascular remodeling in animal models of chronic obstructive pulmonary disease (COPD). The aim of this study was to evaluate the effects of sGC stimulation on oxidative stress in the plasma of guinea pigs chronically exposed to cigarette smoke (CS).

Methods and results

Guinea pigs were exposed to CS or sham for three months, and received either the sGC stimulator BAY 41–2272 or vehicle. Body weight was measured weekly; and markers of oxidative stress in plasma, and airspace size and inflammatory cell infiltrate in lung tissue were analyzed at the end of the study. Compared to sham-exposed guinea pigs, CS-exposed animals gained less body weight and showed higher plasma levels of nitrated tyrosine residues (3-NT), 4-hydroxynonenal (4-HNE), and 8-hydroxydeoxyguanosine (8-OHdG). Treatment with the sGC stimulator led to a body weight gain in the CS-exposed guinea pigs similar to non-exposed and attenuated the increase in 3-NT and 4-HNE. Plasma levels of 3-NT correlated with the severity of inflammatory cell infiltrate in the lung.

Conclusion

Stimulation of sGC prevents oxidative stress induced by CS exposure and is associated with an attenuated inflammatory response in the lung.

OPEN ACCESS

Citation: Paul T, Salazar-Degracia A, Peinado VI, Tura-Ceide O, Blanco I, Barreiro E, et al. (2018) Soluble guanylate cyclase stimulation reduces oxidative stress in experimental Chronic Obstructive Pulmonary Disease. *PLoS ONE* 13(1): e0190628. <https://doi.org/10.1371/journal.pone.0190628>

Editor: Yunchao Su, Augusta University, UNITED STATES

Received: April 21, 2017

Accepted: December 18, 2017

Published: January 5, 2018

Copyright: © 2018 Paul et al. This is an open access article distributed under the terms of the [Creative Commons Attribution License](https://creativecommons.org/licenses/by/4.0/), which permits unrestricted use, distribution, and reproduction in any medium, provided the original author and source are credited.

Data Availability Statement: All relevant data are within the paper and its Supporting Information files.

Funding: The study has been funded by grants from the Instituto de Salud Carlos III (PS09/0536, PI14/00713 and PI16/01147), an unrestricted educational grant from Bayer AG, the Spanish Society of Respiratory Medicine (SEPAR) (24/2015 and /2016) and Catalan Foundation of Pulmonology (FUCAP) (FUCAP 2016).

Cofinanciado por el Fondo Europeo de Desarrollo Regional (FEDER). Unión Europea. “Una manera de hacer Europa”. O. Tura-Ceide was the recipient of IDIBAPS-Biotrack postdoctoral fellowship. The funders had no role in study design, data collection and analysis, decision to publish, or preparation of the manuscript.

Competing interests: With respect the funding from a commercial fund, T. Paul was the recipient of an unrestricted educational grant provided by Bayer AG, Germany. Bayer AG also provided the compound BAY 41-2272 that was used in the experimental studies. Bayer AG did not have any role in the design of the study, the conduction of the experiments, obtaining the results, analysis of the data, drafting the manuscript and/or decision to submit for publication. These contributions do not alter our adherence to PLOS ONE policies on sharing data and materials.

Introduction

Chronic obstructive pulmonary disease (COPD), which is a consequence of cigarette smoking, is one of the most common causes of chronic morbidity and death in the world [1]. It not only affects the respiratory system but also increases the risk of systemic manifestations and serious comorbidities, such as cardiovascular disease, skeletal muscle dysfunction and cachexia [2,3]. These extrapulmonary manifestations further impair quality of life in COPD patients and substantially worsens their prognosis, regardless of the changes occurring in the lung [4–7].

Cigarette smoke (CS) contains harmful substances that produce an inflammatory response and excessive oxidative stress in the lung [8,9]. The spill-over of inflammatory mediators from the lung to the circulation has been postulated as the potential mechanism of the systemic manifestations of COPD [10]. As a source of reactive oxygen species (ROS), this may provoke the oxidation of various biomolecules that generate further reactive molecules when interacting with toxic chemicals in the CS [11]. For instance, levels of ROS-modified proteins, lipid peroxidation, and oxidatively damaged DNA were shown to be elevated in the blood plasma of smokers and patients with COPD [12–14]. These are biomarkers of oxidative damage to skeletal muscle proteins and organs in smokers [15].

Nitric oxide (NO) signaling is essential for many physiological processes and has been proven to be impaired by oxidative stress [16,17]. Under normal conditions, NO activates the key enzyme soluble guanylate cyclase (sGC), which converts guanosine triphosphate (GTP) to cyclic guanosine monophosphate (cGMP). As a second messenger, cGMP controls vascular tone and suppresses smooth muscle proliferation, platelet aggregation, and many other processes [18]. In smokers and patients with COPD, reduced sGC expression, together with compromised function because of oxidation, have been demonstrated in bronchial and alveolar epithelial cells and in airway smooth muscle cells [19,20]. Pharmacologic stimulation of sGC is able to prevent the development of pulmonary hypertension and emphysema in rodent models of COPD [21]. These preventive effects were attributed, at least in part, to the ability of cGMP to reduce inflammatory cell recruitment to the lung and its ability to neutralize damage from oxidative stress by preventing ROS-induced apoptosis and upregulating production of the antioxidant superoxide dismutase (SOD) 1 [21]. Whether the effects of cGMP are limited to the lung or are extended to extrapulmonary organs remains unsettled.

Given its known pulmonary antioxidant properties, it is conceivable that sGC stimulators could have effects on systemic oxidative stress [21]. The present study aimed to evaluate extrapulmonary effects of sGC stimulation in guinea pigs chronically exposed to CS, a well-established experimental model of COPD [22], preventing systemic oxidative stress. We investigated the effects of the sGC stimulator BAY 41–2272 [23] on the formation of ROS and nitrogen species, as measured by identification of well-validated indirect markers of oxidative stress in guinea pig plasma after 3 months of CS exposure. We then studied the relationship between these biomarkers and structural and inflammatory changes in the lung.

Material and methods

Exposure to CS

Thirty-one male Dunkin-Hartley guinea pigs (start weight: 350g–400g, age: 4–5 weeks) were purchased from Harlan Laboratories, Inc. and provided with standard guinea pig chow and water supplemented with ascorbic acid (Bayer Hispania, Sant Joan Despí, Spain) ad libitum in non-metabolic cages. Animals were housed at controlled conditions (temperature: 20–22°C, fixed 12h day/night cycles). After 2 weeks of adaptation, animals were randomly divided into four groups: (1) a sham-exposed control group that received a control vehicle (Polyethylene

glycol 400, 5ml/Kg); Fluka Analytical, Sigma-Aldrich, Steinheim, Germany) ($n = 7$); (2) a sham-exposed treatment group that received the sGC stimulator BAY 41–2272 (provided by Bayer AG, Leverkusen, Germany) ($n = 8$); (3) a CS-exposed control group that received the vehicle only ($n = 7$); and (4) a CS-exposed treatment group that received BAY 41–2272 ($n = 9$). CS exposure was conducted as previously described [21,25,27], with guinea pigs exposed to the smoke of 6 cigarettes (3R4F, Kentucky University Research, Lexington, KY, USA) per day, 5 days a week, for 3 months. After CS exposure, animals received daily doses of either freshly prepared BAY 41–2272 in suspension at a dose of 3 mg/kg by oral gavage or an equivalent amount of the vehicle. Conditions of the guinea pigs were controlled daily before the manipulation and their body weights were measured once per week. Body mass index (BMI) was calculated by dividing the bodyweight by the square of the body length. As the animals tolerated the procedure without complications, application of human endpoints for animals was not necessary. When sacrificed, animals were anesthetized with urethane (2g/kg i.p.; Sigma-Aldrich, Steinheim, Germany) and euthanized by exsanguination. All procedures were approved by the ethics committee for animal experimentation of the University of Barcelona (registry: 2009/5026). An initial set of assessments in these animals have been previously published [22,24–26]

Histological analysis of the lung to validate the experimental model

Methodology for the histologic assessments in the lung have previously been described [21]. Emphysema was assessed by histological hematoxylin staining, measuring the mean linear intercept (MLI) according to standard procedures in 20 randomly selected microscopic fields [21,27]. Inflammatory cells were counted on histological sections stained with hematoxylin and eosin or periodic acid-Schiff, as previously described [21,26]. Intraseptal neutrophils were identified by their segmented nuclei. Cell quantity was related to the septal area, which was measured using Image-Pro Plus software (Media Cybernetics, Inc.). Alveolar macrophages were identified based on their morphology and glycogen content [21]. Results on the preventive effects of BAY 41–2272 on emphysema development and inflammatory cell infiltrate in the lung after CS-exposure have been previously reported [21]. In the present study we analyze the correlation between oxidative stress and such histological assessments.

Oxidative stress markers in blood

Plasma samples were produced by centrifuging EDTA-blood at 2500 RPM for 5 minutes at 4°C. Plasma levels of 3-nitrotyrosine (3-NT), 4-hydroxynonenal (4-HNE), and 8-hydroxydeoxyguanosine (8-OHdG) were assessed by enzyme-linked immunosorbent assays (ELISA; OxiSelect™ Nitrotyrosine ELISA kit, OxiSelect™ HNE Adduct Competitive ELISA kit and OxiSelect™ oxidative DNA Damage ELISA kit, Cell Biolabs, Inc. San Diego, CA, USA) following the manufacturer's instructions and previously reported methodologies [28,29]. Briefly, 50 µL of each sample were added to designated wells and incubated at room temperature for 10 minutes. These samples were then incubated with an additional 50 µL of diluted primary antibody at room temperature for one hour. Thereafter, samples were washed with a wash buffer and incubated with 100 µL of diluted secondary antibody-enzyme conjugate for an additional hour. Finally, the samples were washed several times with a wash buffer and incubated with 100 µL of the substrate solutions for 30 minutes in the dark. The enzyme reaction was stopped by adding 100 µL of a stop solution. A standard curve was always generated for each assay run. Absorbancies were read in a microplate reader (infinite M200, TECAN, Switzerland) at 450 nm using a reference filter of 655 nm.

Plasma biochemical measurements

Total cholesterol, total proteins and triglycerides serum levels were measured using standard enzymatic procedures by the Laboratory of Biochemistry of the Hospital Clínic of Barcelona.

Western blotting

Frozen lung tissue was homogenized (T 10 basic ULTRA-TURRAX®, IKA.) and lysed in a buffer containing 50 mM 4-(2-hydroxyethyl)-1-piperazineethanesulfonic acid (HEPES), 150 mM NaCl, 100 mM sodium fluoride (NaF), 10 mM tetrasodium pyrophosphate ($\text{Na}_4\text{P}_2\text{O}_7$), 5 mM ethylenediaminetetraacetic acid (EDTA), 0.5% Triton-X, 2 $\mu\text{g}/\text{mL}$ leupeptin, 100 $\mu\text{g}/\text{mL}$ phenylmethylsulfonyl fluoride (PMSF), 2 $\mu\text{g}/\text{mL}$ aprotinin, and 10 $\mu\text{g}/\text{mL}$ pepstatin A. Afterwards, samples were centrifuged at 1000g for 30 min and protein levels were determined in the supernatant using the Bradford method (Protein Assay Dye Reagent Concentrate, Bio-rad). 30 μg of total protein were loaded on gels, separated by SDS-PAGE and transferred to polyvinylidene difluoride (PVDF) membranes. Membranes were blocked in 1% BSA and incubated with the primary antibodies overnight (BAX (p19) sc-526, 1:2000 in PBS-Tween; Santa Cruz or GAPDH (FL-355) sc-25778, dilution 1:2000, Santa Cruz). Proteins of interest were indirectly detected using horseradish peroxidase (HRP)-conjugated secondary antibodies (Jackson ImmunoResearch Inc, West Grove, PA, USA) and visualized with a chemiluminescence kit (Thermo scientific, Rockford, IL, USA). Membranes were scanned using the Molecular Imager Chemidoc XRS System (Bio-Rad Laboratories, Hercules, CA, USA) and Quantity One version 4.6.5- software (Bio-Rad Laboratories). All membranes with samples of the different experimental groups were analyzed in the same picture with identical exposure times. Optical densities (OD) of the bands were quantified using the Image Lab- software version 2.0.1 (Bio-Rad Laboratories). ODs of the protein of interest were normalized by the ODs of the loading control GAPDH.

Immunohistochemistry

Paraffin-embedded tissue sections were rehydrated and incubated for 40 min in 1mM EDTA (with 0.05% tween, pH 8) at 95°C. Then, the endogenous peroxidase was blocked with 6% H_2O_2 (in H_2O) for 15min, before slides were incubated for 30 min with the primary antibody (BAX (p19) sc-526, Santa Cruz, 1/20 in PBS) at room temperature. After that, specific proteins were detected with a secondary antibody against primary antibody for 30 min at room temperature and visualized with the Dako REAL™ EnVision™ Detection System (Peroxidase/DAB + Rabbit/Mouse, code k5007, DAKO, Glostrup, Denmark). Nuclei were counterstained with hematoxylin for 2 minutes. After dehydrating and mounting tissue sections in DPX, light microscopy pictures were taken with an Olympus BX 61 microscope (Olympus Corporation, Tokyo, Japan) which was equipped with an image-digitizing camera (Olympus DP 71, Olympus Corporation).

Statistical analysis

Because the study design was two-factorial, each factor with two levels [Factor 1 (CS): CS-exposure vs. non-exposed animals and, Factor 2 (treatment): BAY 41–2272 vs. vehicle only], all experiments were analyzed by two-way analysis of variance (ANOVA) with CS exposure and BAY 41–2272 treatment considered independently when comparing the results between experimental groups. P-values for the independent factors are represented in Tables 1 and 2. To fulfill the assumptions of the two-way ANOVA, data were transformed by forming the square root or natural logarithm to achieve normal distribution of the datasets, if necessary. If

a significant interaction of the two factors was found in the 2-way ANOVA, pairwise multiple comparisons between the experimental groups were performed using Holm–Šidák post-hoc tests and are represented in the text and in the graphs by p-values. To evaluate the potential relationship between study variables, Spearman rank analysis was carried out. In all cases, p-values below 0.05 were considered statistically significant. Missing data of individual animals are related to technical problems and are indicated in the n-numbers below the graphs.

Results

Lung morphometry, body weight, and nutritional status

Guinea pigs exposed to CS developed pulmonary emphysema, as shown by increased MLI ($p < 0.001$ for the comparison of CS+vehicle with sham+vehicle) (Table 1, S1 Fig), and inflammatory cell infiltrate in lung tissue, with evidence of increased numbers of neutrophils in alveolar septa and macrophages in alveolar spaces, as previously reported [21] (Table 1, S2 Fig). Furthermore, CS-exposed animals showed less weight gain compared with the corresponding control group in week 13 (Table 1, Fig 1A); similarly, the BMI at week 13 was significantly decreased in CS-exposed guinea pigs compared with sham-exposed animals (Table 1, Fig 1B).

Treatment with BAY 41–2272 prevented the increase of MLI ($p = 0.002$ for the comparison of CS+vehicle and CS+BAY 41–2272) (Table 1, S1 Fig), and cell infiltrate by neutrophils and macrophages was attenuated (Table 1, S2 Fig). Moreover, the two-way ANOVA revealed a significant interaction between CS exposure and treatment with BAY 41–2272 regarding the extents of emphysema and neutrophilic cell infiltrate (Table 1).

In addition, treatment with BAY 41–2272 almost normalized weight gain among CS-exposed guinea pigs. Body weight at week 13 in the CS+BAY 41–2272 group was similar to the unexposed group, and significantly higher in animals which received treatment (Table 1, Fig 1A). BMI at week 13 was significantly higher in CS-exposed guinea pigs that received BAY 41–2272 when compared to CS-exposed animals that received vehicle (Table 1, Fig 1B).

Table 1. Changes in emphysema extent, lung inflammation, plasma oxidative stress, apoptosis and bodyweight associated with BAY 41–2272 treatment in guinea pigs chronically exposed to CS.

	Mean ± SD				2-way ANOVA		
	Sham + Vehicle	Sham + BAY 41–2272	CS + Vehicle	CS + BAY 41–2272	Effect of CS	Effect of BAY 41–2272	Interaction between CS & BAY 41–2272
Mean Linear Intercept (µm)	58 ± 4	59 ± 6	74 ± 6	62 ± 8	$p < 0.001$	$p = 0.05$	$p = 0.008$
Neutrophils (x10 ⁻⁷ cells/µm ²)	1.61 ± 0.7	1.88 ± 0.52	4.17 ± 1.66	1.73 ± 0.59	$p = 0.004$	$p = 0.02$	$p = 0.001$
Macrophages (cells/field)	0.81 ± 0.08	0.57 ± 0.2	1.33 ± 0.24	0.94 ± 0.15	$p < 0.001$	$p < 0.001$	$p = 0.27$
NT (nM)	8.7 ± 5.4	8.3 ± 4.8	21.7 ± 15.3	7.0 ± 4.9	$p = 0.16$	$p = 0.02$	$p = 0.03$
4-HNE (µg/ml)	1.9 ± 1.0	2.6 ± 1.4	6.7 ± 4.5	2.4 ± 1.6	$p = 0.06$	$p = 0.19$	$p = 0.029$
8-OHdG (ng/ml)	2.2 ± 0.4	2.6 ± 0.4	4.3 ± 2.4	3.3 ± 1.1	$p = 0.006$	$p = 0.51$	$p = 0.19$
BMI (kg/m ²)	9.41 ± 0.53	9.89 ± 0.54	8.42 ± 0.51	9.03 ± 0.58	$p < 0.001$	$p = 0.009$	$p = 0.737$
Bodyweight week 13 (g)	918.29 ± 57.37	976.88 ± 75.09	802.00 ± 57.37	873.11 ± 85.36	$p < 0.001$	$p = 0.021$	$p = 0.815$
BAX/GAPDH ratio (OD)	0.12 ± 0.04	0.13 ± 0.03	0.32 ± 0.08	0.2 ± 0.06	$p < 0.001$	$p = 0.015$	$p = 0.003$

CS = cigarette smoke, 3-NT = 3-nitrotyrosine, 4-HNE = 4-hydroxynonenal, 8-OHdG = 8-hydroxydeoxyguanosine, BMI = body mass index, GAPDH = Glyceraldehyde 3-phosphate dehydrogenase, OD = optical density. Values are expressed as mean ± SD in the different experimental groups. Statistical differences were analyzed by 2-way ANOVA. Effects of CS exposure, BAY 41–2272 treatment, and their interaction, respectively, are represented at the right of the table.

<https://doi.org/10.1371/journal.pone.0190628.t001>

Table 2. Changes in nutritional status associated with BAY 41–2272 treatment in guinea pigs chronically exposed to CS.

	Mean ± SD				2-way ANOVA		
	Sham + Vehicle	Sham + BAY 41–2272	CS + Vehicle	CS + BAY 41–2272	Effect of CS	Effect of BAY 41–2272	Interaction between CS & BAY 41–2272
Protein (g/L)	41 ± 5	45 ± 2	43 ± 4	46 ± 4	0.37	0.03	0.91
Triglyceride (mg/dL)	185 ± 80	157 ± 31	159 ± 90	187 ± 105	0.69	0.97	0.49
Cholesterol (mg/dL)	42 ± 18	42 ± 7	44 ± 18	43 ± 13	0.79	0.91	0.82

Representation of the mean ± SD in the different experimental groups. Statistical differences were analyzed by 2-way ANOVA. Effects of CS exposure, BAY 41–2272 treatment, and their interaction, respectively, are represented at the right of the table.

<https://doi.org/10.1371/journal.pone.0190628.t002>

To further examine the impact of treatment with BAY 41–2272 on the nutritional status, we analyzed serum protein, triglyceride and cholesterol levels. While triglycerides and cholesterol levels did not differ from unexposed animals in the groups receiving BAY 41–2272, protein levels were significantly higher guinea pigs treated with BAY 41–2272 (Table 2, S3 Fig).

Markers of oxidative stress in the plasma

Compared with sham-exposed animals, CS-exposed guinea pigs had significantly higher plasma levels of 3-NT ($p = 0.02$), 4-HNE ($p = 0.008$), and 8-OHdG (Table 1, Fig 2). Treatment with BAY 41–2272 prevented the increase of both 3-NT ($p = 0.002$) and 4-HNE ($p = 0.02$) as compared with non treated CS-exposed animals. Furthermore, the levels of both molecules did not differ from those in sham-exposed animals, and the interaction between CS exposure and BAY 41–2272 treatment was statistically significant in the two-way ANOVA (Fig 2A and 2B, Table 1). Regarding 8-OHdG levels, a slight decrease was observed in CS exposed animals after treatment with BAY 41–2272 but did not reach statistical significance (Table 1, Fig 2C).

Associations between plasma levels of oxidative stress markers and inflammatory cell infiltrates in the lung

Plasma levels of 3-NT were significantly associated with the number of inflammatory cells in the lungs (intraseptal neutrophils, $R = 0.501$; $p = 0.007$) throughout all study groups.

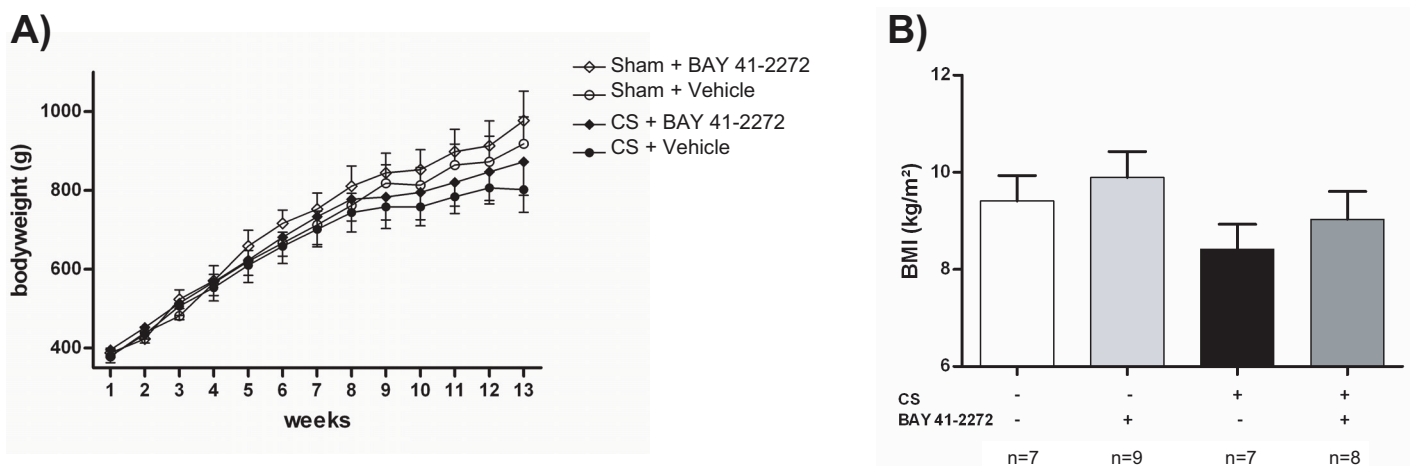


Fig 1. Body weight evolution in the different experimental groups (A). Statistical differences were analyzed by 2-way ANOVA and are shown in Table 1. (B) Body mass index at week 13. All data are represented as mean ± SD.

<https://doi.org/10.1371/journal.pone.0190628.g001>

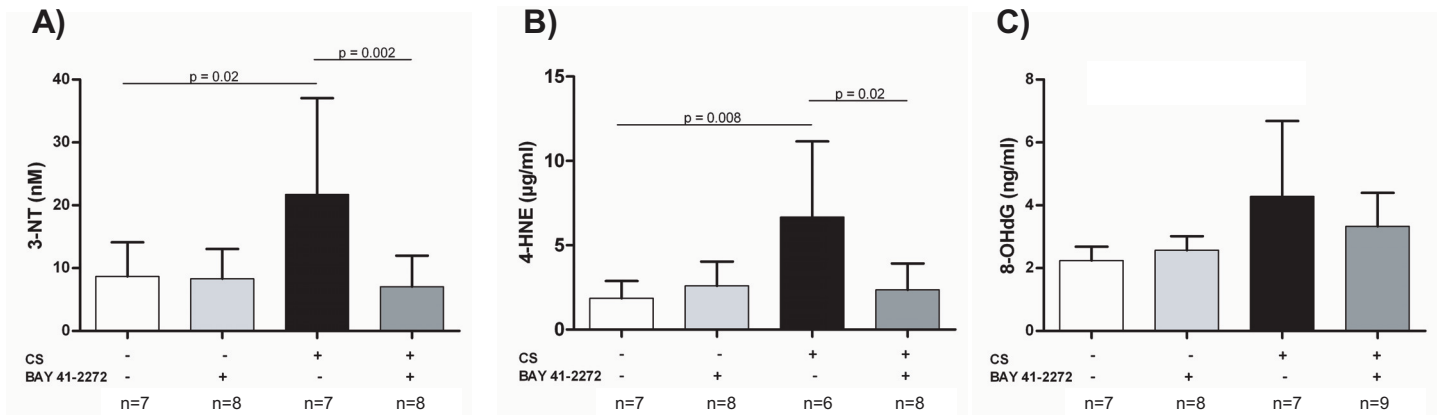


Fig 2. Effects of soluble guanylate cyclase (sGC) stimulation on plasma markers of oxidative stress. Guinea pigs were exposed to either cigarette smoke (CS) or sham for 3 months, and received either the sGC stimulator (BAY 41–2272) or vehicle only. (A) Presence of nitrated tyrosine residues (3-NT), (B) 4-hydroxynonenal, and (C) 8-hydroxydeoxyguanosine were quantified by enzyme-linked immunosorbent assay (mean ± SD). Statistical differences were analyzed by 2-way ANOVA. Pairwise multiple comparisons between the individual groups were performed using the Holm–Šidák method.

<https://doi.org/10.1371/journal.pone.0190628.g002>

Moreover, a correlation trend of 3-NT levels with lung macrophages was observed ($R = 0.35$; $p = 0.056$) (Fig 3). Plasma levels of 8-OHdG and 4-HNE did not correlate significantly with either the number of neutrophils or macrophages in the lungs (data not shown).

Impact of BAY 41–2272 on the regulation of apoptosis in lung tissue

Protein levels of the pro-apoptotic regulator BAX were significantly increased in animals exposed to CS ($p < 0.001$) when compared to controls (Fig 4A and Table 1). Treatment with the sGC-stimulator BAY 41–2272 reduced BAX protein expression as analyzed by western blot ($p < 0.001$ for CS+Vehicle vs. CS+BAY 41–2272) (Fig 4A and 4B). Likewise, representative immunohistochemically stained lung tissue sections showed lower levels of BAX in CS-exposed animals which were treated with the sGC-stimulator when compared to CS-exposed guinea pigs which did not receive the treatment (Fig 4C).

Discussion

Through the analysis of blood biomarkers, this study shows that the sGC stimulator BAY 41–2272 administered to guinea pigs chronically exposed to CS can prevent oxidative stress in the plasma.

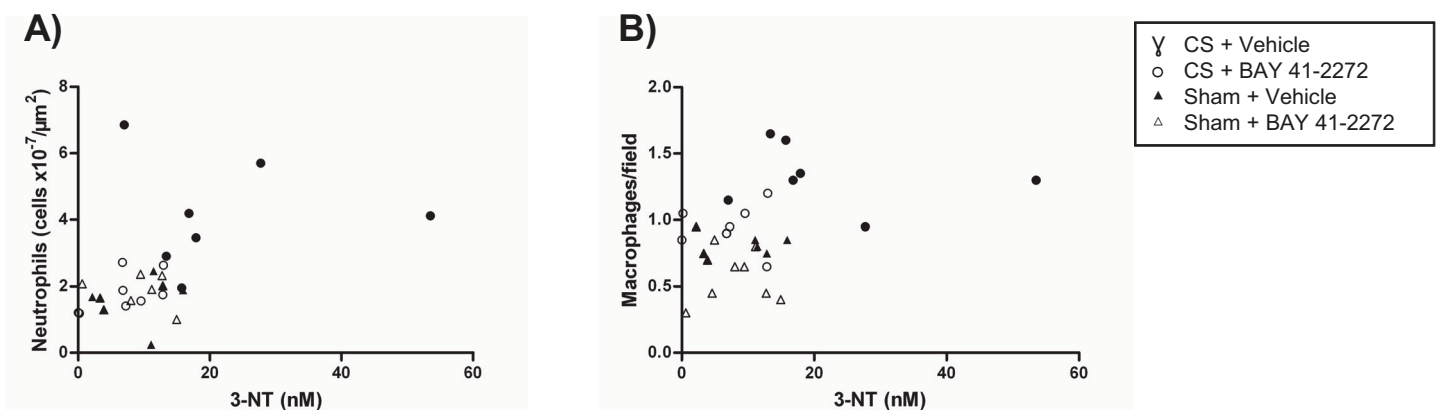


Fig 3. Correlation analysis of inflammatory cell infiltrate in the lungs (counted on histological sections) and plasma levels of oxidative stress markers. Spearman rank correlation was used to evaluate the relationship between (A) intraseptal neutrophils (cells $\times 10^{-7}/\mu\text{m}^2$) $R = 0.501$, $p = 0.007$ and (B) macrophages (cells/field) $R = 0.35$, $p = 0.056$ and 3-NT. Assessment was by enzyme-linked immunosorbent assay.

<https://doi.org/10.1371/journal.pone.0190628.g003>

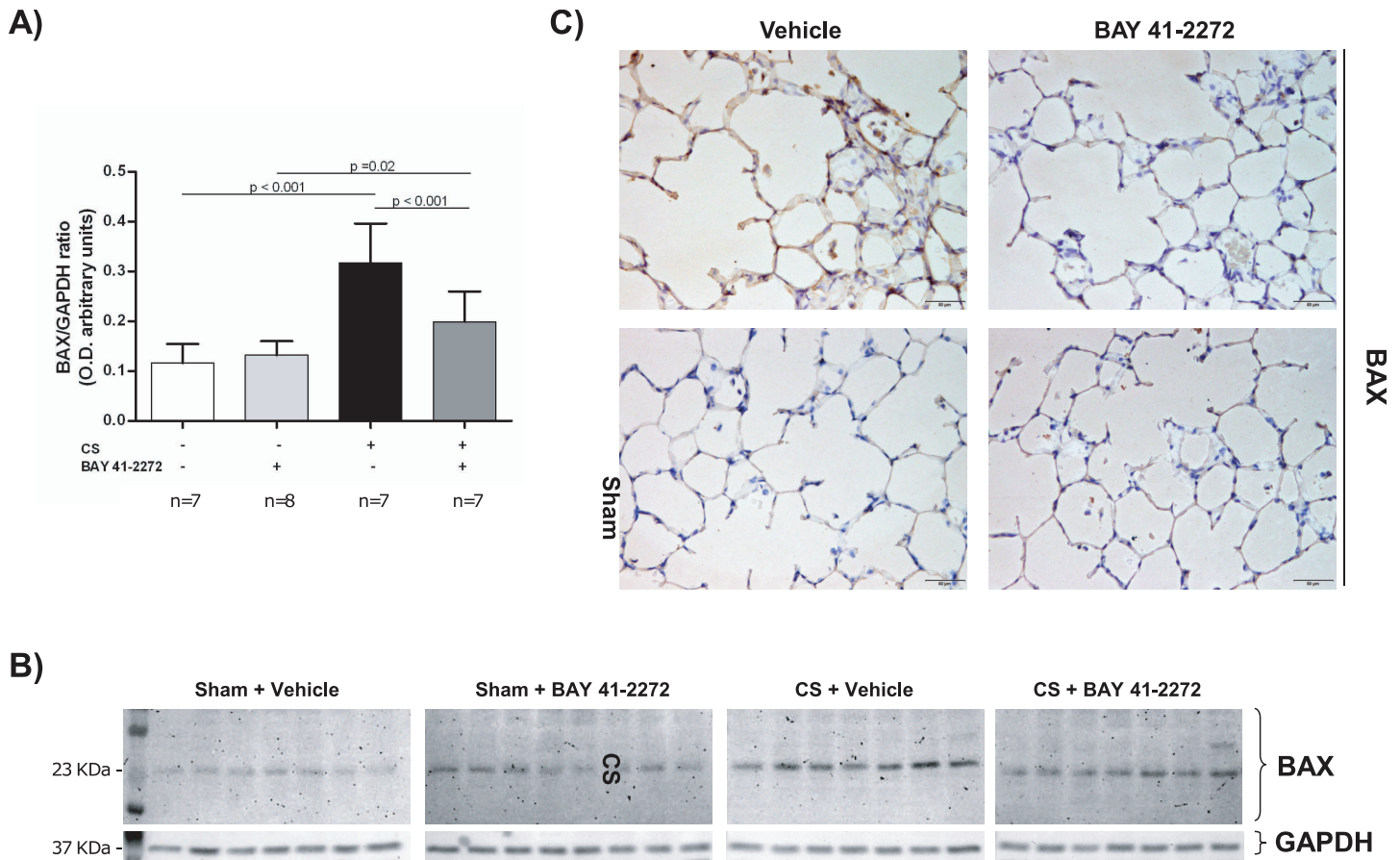


Fig 4. Effects of soluble guanylate cyclase stimulation on the regulation of apoptosis. Guinea pigs were exposed to either cigarette smoke (CS) or sham for 3 months, and received either the sGC stimulator (BAY 41–2272) or vehicle only. (A) Protein expression of BAX was measured by western blot (A and B) and immunohistochemistry (C). Statistical differences in western blotting results were analyzed by 2-way ANOVA. Pairwise multiple comparisons between the individual groups were performed using the Holm–Sidak method.

<https://doi.org/10.1371/journal.pone.0190628.g004>

In a previous publication we showed beneficial effects of sGC stimulation on emphysema development, which could be partially explained by the ability of this class of drugs to inhibit the induction of apoptosis, to increase antioxidant enzymes, and to stimulate mediators of vascular and tissue integrity. Moreover, an attenuation of inflammation by BAY 41–2272 was discussed to contribute to the prevention of emphysema development [21]. Consistent with these results in the present study we observed a significant relationship between the plasma levels of oxidatively damaged proteins (3-NT) and inflammatory cells in the lung. However, besides the abnormal inflammatory response present in the lungs, COPD is associated with systemic inflammation that includes augmentation of pro-inflammatory cytokines, the activation of inflammatory cells, and the development of oxidative stress in the circulation [30]. Our data indicate that in this experimental model, treatment with sGC stimulators is able to correct both pulmonary damage and systemic oxidant/antioxidant imbalances.

In guinea pigs, chronic CS exposure has previously been shown to induce transient, but repetitive, systemic oxidative damage that has been considered responsible for impaired metabolism and a reduced capacity of CS-exposed animals to gain body weight [31]. To find evidence in support of this concept, we analyzed oxidative stress biomarkers (e.g., 3-NT, 4-HNE, and 8-OHdG) in plasma samples, and demonstrated that plasma oxidative damage

was significantly increased by 3 months of CS exposure. By mediating a number of downstream mechanisms and compromising normal cell function, these molecules contribute to the progression of the pulmonary and systemic features of COPD [32,33].

In line with our results, a trend has been shown for levels of TNF- α to increase in the circulation and for plasma lipid peroxidation to increase acutely in guinea pigs after 6 months of CS exposure [31]. Treatment with BAY 41–2272 attenuated the effects of CS exposure on plasma levels of NT and 4-HNE in the present study. In pulmonary arterial hypertension, the NO–cGMP axis has been shown to be involved in modulating the inflammatory and redox status, with evidence that clinical improvement after sildenafil treatment was, at least in part, attributable to a reduction of plasma 4-HNE levels [34]. In alveolar epithelial and endothelial cells, sGC stimulation inhibits ROS-induced apoptosis and enhances SOD1 expression (an ROS scavenger) [21]. The reduction in ROS damage and increase in antioxidant defense might explain the plasma effects of the sGC stimulator in this study. Moreover, excessive oxidative stress contributes to impaired NO-signaling, because high concentrations of 4-HNE have been shown to cause eNOS-uncoupling, resulting in reduced NO bioavailability [35]. Accordingly, stimulation of sGC by BAY 41–2272 may help preserve the physiological functions of the NO pathway under conditions of oxidative stress.

Whether systemic inflammation and oxidative stress in COPD are consequences of pulmonary impairment or they represent independent features remain a matter of debate [36–38]. A proposed hypothesis for the origin of systemic features is the so called *spill-over* of local inflammatory events in the lungs to the circulation [10,39]. In support of this hypothesis, we found a positive correlation between plasma 3-NT levels and neutrophilic granulocytes, with a trend toward a positive correlation with macrophages in the lung. In addition, there is evidence that neutrophils, circulating monocytes and macrophages of patients with COPD function abnormally, being capable of producing more ROS and inflammatory mediators than those of healthy individuals [40–42]. Through increased peroxynitrite production, for instance, this may give rise to the observed protein modifications in the CS-exposed animals in the present study.

It is well known that chronic hypoxemia may cause systemic inflammation, and that this may add to the effects of lung inflammation associated with COPD [43]. In fact, it has been observed that the degree of hypoxemia correlates with plasma inflammatory markers [44]. Hence, the ability of sGC stimulation to prevent both emphysema and inflammatory infiltration in the lungs could produce synergistic effects, resulting in fewer products of ROS damage in plasma. Supporting previous explanations regarding protective effects of sGC stimulators on apoptosis [21], we also found a decrease in the pro-apoptotic BAX protein in CS-exposed animals treated with the drug. A negative regulation of apoptosis upon sGC-stimulator treatment might additionally explain the favourable effects of this substance class on emphysema development. Consistent with these findings, we also observed that both body weight gain and BMI were reduced in the CS-exposed animals compared with the non-exposed controls. This hints at a systemically impaired equilibrium in CS exposed animals. In the same animals, we observed that intervention with BAY 41–2272 compensated for weight and BMI issues seen in CS-exposed animals. Blood protein levels were elevated during treatment with BAY 41–2272 as well, allowing for the assumption that stimulation of sGC signaling exerts additional effects to those already described for the lung [21]. Interestingly, similar effects on body weight gain have been observed in guinea pigs chronically exposed to CS and treated with sildenafil [27] further supporting the role of cGMP in body weight gain.

Our experiments have limitations. Notably, we used a preventive treatment design, so the effects of sGC stimulation in a therapeutic setting, after the manifestation of COPD symptoms, cannot be extrapolated based on our results. This will need to be addressed in future studies

with a therapeutic design. In addition, further evaluation of plasma inflammation would have been useful to help place our results concerning ROS damage in context. Currently, though, there are few commercial antibodies against guinea pig proteins, and with several different antibodies we could not detect inflammatory markers in the plasma of our subjects. Furthermore, we used a relatively low dose (3 mg/kg) of BAY 41–2272. We cannot rule out that a higher dose might have possibly revealed stronger effects, particularly on 8-OHdG formation. It is also likely that a greater number of animals would have increased the statistical power. Even though we previously found beneficial effects of the drug on emphysema development and lung inflammation, an improvement of lung function (measured by wholebody plethysmography) was not observed [21]. Similarly, even though the evaluated markers reflect oxidative stress conditions reliably, our results cannot be translated directly into functional limitations in the animals. For that reason, measuring exercise capacity would have been useful, but would have added considerable complexity to our study design.

In conclusion, the present study shows that the sGC stimulator BAY 41–2272 can prevent oxidative stress in the plasma in a validated guinea pig model of COPD. Whether these antioxidant properties result from diminished inflammation in the lung after sGC treatment or whether they denote a direct extrapulmonary effect needs to be addressed in future investigations. Our results would imply that targeting oxidative stress in COPD might not only be beneficial for treating pulmonary symptoms but also for preventing or improving its systemic manifestations.

Supporting information

S1 Fig. Mean chord length quantification between alveolar septa (A). Data are represented as dot plots with mean and standard deviation. (B) Representative histology from guinea pig lungs (HE-staining). (C) Magnified image detail of the original photographs shown in (B) (frames). Scale bar: 100µm. For statistics see [Table 1](#) in the main manuscript. (EPS)

S2 Fig. Recruitment of neutrophils (A) and macrophages (C) to the lung tissue. Data are represented as dot plots with mean and standard deviation. Representative histology of neutrophils (HE-staining, (B)) and macrophages (PAS-staining, (D)) and corresponding magnified image details of the original pictures (frames). For statistics see [Table 1](#) in the main manuscript. (EPS)

S3 Fig. Changes in nutritional status associated with BAY 41–2272 treatment in guinea pigs chronically exposed to CS. Dot plot of individual values for plasma protein, triglycerides and cholesterol. Also is shown the median and range interquartile. For statistics see [Table 2](#) in the main manuscript. (EPS)

Acknowledgments

We thank Cristina Bonjoch for their expert technical assistance. The authors also thank Michael Maudsley for English revision on the manuscript. This work was developed at the Centre de Recerca Biomèdica Cellex, Barcelona, Spain.

Author Contributions

Conceptualization: Victor I. Peinado, Esther Barreiro, Joan A. Barberà.

Formal analysis: Tanja Paul, Anna Salazar-Degracia, Victor I. Peinado, Olga Tura-Ceide, Isabel Blanco.

Funding acquisition: Victor I. Peinado, Esther Barreiro, Joan A. Barberà.

Methodology: Tanja Paul, Anna Salazar-Degracia, Victor I. Peinado, Esther Barreiro.

Project administration: Victor I. Peinado.

Supervision: Victor I. Peinado, Esther Barreiro, Joan A. Barberà.

Validation: Tanja Paul, Victor I. Peinado.

Writing – original draft: Tanja Paul, Victor I. Peinado.

Writing – review & editing: Victor I. Peinado, Olga Tura-Ceide, Isabel Blanco, Esther Barreiro, Joan A. Barberà.

References

1. López-Campos JL, Tan W, Soriano JB. Global burden of COPD. *Respirology*. 2016; 21: 14–23. <https://doi.org/10.1111/resp.12660> PMID: 26494423
2. Murali Mohan BV, Sen T, Ranganath R. Systemic manifestations of COPD. *J Assoc Physicians India*. 2012; 60 Suppl: 44–47.
3. Negewo NA, Gibson PG, McDonald VM. COPD and its comorbidities: Impact, measurement and mechanisms. *Respirology*. 2015; 20: 1160–1171. <https://doi.org/10.1111/resp.12642> PMID: 26374280
4. Hillas G, Perlikos F, Tsiligianni I, Tzanakis N. Managing comorbidities in COPD. *Int J Chron Obstruct Pulmon Dis*. 2015; 10: 95–109. <https://doi.org/10.2147/COPD.S54473> PMID: 25609943
5. Barreiro E, Bustamante V, Cejudo P, Gáldiz JB, Gea J, de Lucas P, et al. Guidelines for the evaluation and treatment of muscle dysfunction in patients with chronic obstructive pulmonary disease. *Arch Bronconeumol*. 2015; 51: 384–395. <https://doi.org/10.1016/j.arbres.2015.04.011> PMID: 26072153
6. Maltais F, Decramer M, Casaburi R, Barreiro E, Burelle Y, Debigaré R, et al. An official American Thoracic Society/European Respiratory Society statement: update on limb muscle dysfunction in chronic obstructive pulmonary disease. *Am J Respir Crit Care Med*. 2014; 189: e15–62. <https://doi.org/10.1164/rccm.201402-0373ST> PMID: 24787074
7. Barreiro E. Skeletal Muscle Dysfunction in COPD: Novelties in The Last Decade. *Arch Bronconeumol*. 2017; 53: 43–44. <https://doi.org/10.1016/j.arbres.2016.07.009> PMID: 27641307
8. Talhout R, Schulz T, Florek E, van Benthem J, Wester P, Opperhuizen A. Hazardous Compounds in Tobacco Smoke. *Int J Environ Res Public Health*. 2011; 8: 613–628. <https://doi.org/10.3390/ijerph8020613> PMID: 21556207
9. Fischer BM, Voynow JA, Ghio AJ. COPD: balancing oxidants and antioxidants. *Int J Chron Obstruct Pulmon Dis*. 2015; 10: 261–276. <https://doi.org/10.2147/COPD.S42414> PMID: 25673984
10. Barnes PJ, Celli BR. Systemic manifestations and comorbidities of COPD. *Eur Respir J*. 2009; 33: 1165–1185. <https://doi.org/10.1183/09031936.00128008> PMID: 19407051
11. Ho E, Karimi Galougahi K, Liu C-C, Bhindi R, Figtree GA. Biological markers of oxidative stress: Applications to cardiovascular research and practice. *Redox Biol*. 2013; 1: 483–491. <https://doi.org/10.1016/j.redox.2013.07.006> PMID: 24251116
12. Woźniak A, Górecki D, Szpinda M, Mila-Kierzenkowska C, Woźniak B. Oxidant-Antioxidant Balance in the Blood of Patients with Chronic Obstructive Pulmonary Disease After Smoking Cessation. *Oxid Med Cell Longev*. 2013; 2013. <https://doi.org/10.1155/2013/897075> PMID: 24089631
13. Zinellu E, Zinellu A, Fois AG, Carru C, Pirina P. Circulating biomarkers of oxidative stress in chronic obstructive pulmonary disease: a systematic review. *Respir Res*. 2016; 17. <https://doi.org/10.1186/s12931-016-0471-z> PMID: 27842552
14. Hartmann SE, Pialoux V, Leigh R, Poulin MJ. Decreased cerebrovascular response to CO₂ in postmenopausal females with COPD: role of oxidative stress. *Eur Respir J*. 2012; 40: 1354–1361. <https://doi.org/10.1183/09031936.00197211> PMID: 22496327
15. Barreiro E, Peinado VI, Galdiz JB, Ferrer E, Marin-Corral J, Sánchez F, et al. Cigarette smoke-induced oxidative stress: A role in chronic obstructive pulmonary disease skeletal muscle dysfunction. *Am J Respir Crit Care Med*. 2010; 182: 477–488. <https://doi.org/10.1164/rccm.200908-1220OC> PMID: 20413628

16. Ghimire K, Altmann HM, Straub AC, Isenberg JS. Nitric oxide: what's new to NO? *Am J Physiol—Cell Physiol.* 2017; 312: C254–C262. <https://doi.org/10.1152/ajpcell.00315.2016> PMID: 27974299
17. Gerassimou C, Kotanidou A, Zhou Z, Simoes DCM, Simoes DDC, Roussos C, et al. Regulation of the expression of soluble guanylyl cyclase by reactive oxygen species. *Br J Pharmacol.* 2007; 150: 1084–1091. <https://doi.org/10.1038/sj.bjp.0707179> PMID: 17339839
18. Stasch J-P, Pacher P, Evgenov OV. Soluble Guanylate Cyclase as an Emerging Therapeutic Target in Cardiopulmonary Disease. *Circulation.* 2011; 123: 2263–2273. <https://doi.org/10.1161/CIRCULATIONAHA.110.981738> PMID: 21606405
19. Glynos C, Dupont LL, Vassilakopoulos T, Papapetropoulos A, Brouckaert P, Giannis A, et al. The role of soluble guanylyl cyclase in chronic obstructive pulmonary disease. *Am J Respir Crit Care Med.* 2013; 188: 789–799. <https://doi.org/10.1164/rccm.201210-1884OC> PMID: 23841447
20. Dupont LL, Glynos C, Bracke KR, Brouckaert P, Brusselle GG. Role of the nitric oxide-soluble guanylyl cyclase pathway in obstructive airway diseases. *Pulm Pharmacol Ther.* 2014; 29: 1–6. <https://doi.org/10.1016/j.pupt.2014.07.004> PMID: 25043200
21. Weissmann N, Lobo B, Pichl A, Parajuli N, Seimetz M, Puig-Pey R, et al. Stimulation of soluble guanylate cyclase prevents cigarette smoke-induced pulmonary hypertension and emphysema. *Am J Respir Crit Care Med.* 2014; 189: 1359–1373. <https://doi.org/10.1164/rccm.201311-2037OC> PMID: 24738736
22. Wright JL, Churg A. A model of tobacco smoke-induced airflow obstruction in the guinea pig. *Chest.* 2002; 121: 188S–191S. PMID: 12010849
23. Evgenov OV, Pacher P, Schmidt PM, Haskó G, Schmidt HHHW, Stasch J-P. NO-independent stimulators and activators of soluble guanylate cyclase: discovery and therapeutic potential. *Nat Rev Drug Discov.* 2006; 5: 755–768. <https://doi.org/10.1038/nrd2038> PMID: 16955067
24. Wright JL, Churg A. Cigarette smoke causes physiologic and morphologic changes of emphysema in the guinea pig. *Am Rev Respir Dis.* 1990; 142: 1422–1428. https://doi.org/10.1164/ajrccm/142.6_Pt_1.1422 PMID: 2252262
25. Ferrer E, Peinado VI, Díez M, Carrasco JL, Musri MM, Martínez A, et al. Effects of cigarette smoke on endothelial function of pulmonary arteries in the guinea pig. *Respir Res.* 2009; 10: 76. <https://doi.org/10.1186/1465-9921-10-76> PMID: 19682386
26. Domínguez-Fandos D, Peinado VI, Puig-Pey R, Ferrer E, Musri MM, Ramírez J, et al. Pulmonary inflammatory reaction and structural changes induced by cigarette smoke exposure in the Guinea pig. *COPD.* 2012; 9: 473–484. <https://doi.org/10.3109/15412555.2012.691999> PMID: 22708688
27. Domínguez-Fandos D, Valdés C, Ferrer E, Puig-Pey R, Blanco I, Tura-Ceide O, et al. Sildenafil in a cigarette smoke-induced model of COPD in the guinea-pig. *Eur Respir J.* 2015; 46: 346–354. <https://doi.org/10.1183/09031936.00139914> PMID: 25929951
28. Puig-Vilanova E, Rodríguez DA, Lloreta J, Ausin P, Pascual-Guardia S, Broquetas J, et al. Oxidative stress, redox signaling pathways, and autophagy in cachectic muscles of male patients with advanced COPD and lung cancer. *Free Radic Biol Med.* 2015; 79: 91–108. <https://doi.org/10.1016/j.freeradbiomed.2014.11.006> PMID: 25464271
29. Barreiro E, Femoselle C, Mateu-Jimenez M, Sánchez-Font A, Pijuan L, Gea J, et al. Oxidative stress and inflammation in the normal airways and blood of patients with lung cancer and COPD. *Free Radic Biol Med.* 2013; 65: 859–871. <https://doi.org/10.1016/j.freeradbiomed.2013.08.006> PMID: 23954470
30. Barnes PJ. Inflammatory mechanisms in patients with chronic obstructive pulmonary disease. *J Allergy Clin Immunol.* 2016; 138: 16–27. <https://doi.org/10.1016/j.jaci.2016.05.011> PMID: 27373322
31. Ardite E, Peinado VI, Rabinovich RA, Fernández-Checa JC, Roca J, Barberà JA. Systemic effects of cigarette smoke exposure in the guinea pig. *Respir Med.* 2006; 100: 1186–1194. <https://doi.org/10.1016/j.rmed.2005.10.023> PMID: 16330198
32. Van Eeden SF, Sin DD. Oxidative stress in chronic obstructive pulmonary disease: A lung and systemic process. *Can Respir J J Can Thorac Soc.* 2013; 20: 27–29.
33. Kirkham PA, Barnes PJ. Oxidative stress in COPD. *Chest.* 2013; 144: 266–273. <https://doi.org/10.1378/chest.12-2664> PMID: 23880677
34. Semen K, Yelisyeyeva O, Jarocka-Karpowicz I, Kaminskyy D, Solovey L, Skrzydlewska E, et al. Sildenafil reduces signs of oxidative stress in pulmonary arterial hypertension: Evaluation by fatty acid composition, level of hydroxynonenal and heart rate variability. *Redox Biol.* 2016; 7: 48–57. <https://doi.org/10.1016/j.redox.2015.11.009> PMID: 26654977
35. Whitsett J, Picklo MJ, Vasquez-Vivar J. 4-Hydroxy-2-Nonenal Increases Superoxide Anion Radical in Endothelial Cells via Stimulated GTP Cyclohydrolase Proteasomal Degradation. *Arterioscler Thromb Vasc Biol.* 2007; 27: 2340–2347. <https://doi.org/10.1161/ATVBAHA.107.153742> PMID: 17872449

36. Tkacova R. Systemic Inflammation in Chronic Obstructive Pulmonary Disease: May Adipose Tissue Play a Role? Review of the Literature and Future Perspectives. *Mediators Inflamm.* 2010; 2010: e585989. <https://doi.org/10.1155/2010/585989> PMID: 20414465
37. Barker BL, McKenna S, Mistry V, Pancholi M, Patel H, Haldar K, et al. Systemic and pulmonary inflammation is independent of skeletal muscle changes in patients with chronic obstructive pulmonary disease. *Int J Chron Obstruct Pulmon Dis.* 2014; 9: 975–981. <https://doi.org/10.2147/COPD.S63568> PMID: 25246784
38. Sinden NJ, Stockley RA. Systemic inflammation and comorbidity in COPD: a result of “overspill” of inflammatory mediators from the lungs? Review of the evidence. *Thorax.* 2010; 65: 930–936. <https://doi.org/10.1136/thx.2009.130260> PMID: 20627907
39. Agustí AGN, Noguera A, Sauleda J, Sala E, Pons J, Busquets X. Systemic effects of chronic obstructive pulmonary disease. *Eur Respir J.* 2003; 21: 347–360. <https://doi.org/10.1183/09031936.03.00405703> PMID: 12608452
40. Noguera A, Batle S, Miralles C, Iglesias J, Busquets X, MacNee W, et al. Enhanced neutrophil response in chronic obstructive pulmonary disease. *Thorax.* 2001; 56: 432–437. <https://doi.org/10.1136/thorax.56.6.432> PMID: 11359957
41. Vlahos R, Bozinovski S. Role of Alveolar Macrophages in Chronic Obstructive Pulmonary Disease. *Front Immunol.* 2014; 5. <https://doi.org/10.3389/fimmu.2014.00435> PMID: 25309536
42. McGuinness AJA, Sapey E. Oxidative Stress in COPD: Sources, Markers, and Potential Mechanisms. *J Clin Med.* 2017; 6: 21. <https://doi.org/10.3390/jcm6020021> PMID: 28212273
43. Kent BD, Mitchell PD, McNicholas WT. Hypoxemia in patients with COPD: cause, effects, and disease progression. *Int J Chron Obstruct Pulmon Dis.* 2011; 6: 199–208. <https://doi.org/10.2147/COPD.S10611> PMID: 21660297
44. Takabatake N, Nakamura H, Abe S, Inoue S, Hino T, Saito H, et al. The relationship between chronic hypoxemia and activation of the tumor necrosis factor- α system in patients with chronic obstructive pulmonary disease. *Am J Respir Crit Care Med.* 2000; 161: 1179–1184. <https://doi.org/10.1164/ajrcm.161.4.9903022> PMID: 10764309